Energy-Gain Measurements from a Microwave Inverse Free-Electron-Laser Accelerator

R. B. Yoder,[1,*] T. C. Marshall,[2] and J. L. Hirshfield[1,3]

[1]*Physics Department, Yale University, New Haven, Connecticut 06520-8124*
[2]*Department of Applied Physics, Columbia University, New York, New York 10027*
[3]*Omega-P, Inc., 345 Whitney Avenue, Suite 100, New Haven, Connecticut 06511*

(Received 17 October 2000)

Experiments are reported on inverse free-electron-laser acceleration, including for the first time observations of the energy change as a function of relative injection phase of the electron bunches. The microwave accelerating structure consists of a uniform circular waveguide with a helical wiggler and an axial magnetic field. Acceleration of the entire beam by 6% is seen for 6 MeV electron bunches at optimum relative phase. Experimental results compare favorably, for accelerating phases, with predictions of a three-dimensional simulation that includes large-orbit effects.

DOI: 10.1103/PhysRevLett.86.1765 PACS numbers: 41.75.Lx, 41.60.Cr

Inverse free-electron lasers (IFELs) were first described in the 1970s [1] and have been proposed for future high-gradient particle accelerators [2]. The IFEL is a promising stageable vacuum laser accelerator of electrons or positrons, based on existing technology, with possible gradients in the 100–400 MeV/m range [3]. In the past decade several prototypes have been operated [4,5] and compared with a one-dimensional theory of the interaction [6], and the physics of IFEL staging is currently being investigated at Brookhaven National Laboratory [7]. We report here on experiments using a prototype IFEL accelerator in which we compare the large-orbit behavior of the IFEL to detailed numerical predictions using a fully three-dimensional theory. Such a theory is required to analyze future compact high-energy IFEL devices, as particle orbits at the energies proposed would necessarily be comparable to the beam waist of the accelerating field.

The IFEL interaction, in which the coupling of a periodic magnetic field and an electromagnetic wave can accelerate electrons and positrons, was first demonstrated in 1992 in the millimeter-wave regime [4]; however, there were reports of stimulated absorption by an electron beam in connection with early FEL experiments [8], implying small energy gain by electrons [9]. More recently a series of experiments using a 10-μm, 1–5-GW laser have shown maximal energy increase approaching 5% for an injected energy of 40 MeV [5] as well as beam bunching at the optical wavelength scale [6]. The experiments described here use microwave power at $f = 2.8$ GHz and allow electrons to be injected at a single value of the ponderomotive phase, enabling direct observation of the phase response of the IFEL; this process was not demonstrated in any previous experiment. As predicted by theory and three-dimensional simulation [10], the measured energy change is strongly phase dependent but asymmetric for the configuration described here, since the helical wiggler employed is tapered in period.

An approximate one-dimensional treatment [3] of the IFEL acceleration process for a constant-period wiggler predicts an energy gain rate

$$\frac{d\gamma}{dz} = \frac{2\pi a_s a_w}{\gamma \lambda_s} \sin\Phi , \tag{1}$$

which is independent of charge sign, where γ is the relativistic energy factor, λ_s is the free-space wavelength of the driving electromagnetic radiation, $a_s = eE_0\lambda_s/2\pi mc^2$ is the normalized electric field strength in the structure, E_0 is the electric field amplitude of the radiation, and $a_w = eB_w\lambda_w/2\pi mc$ is the normalized wiggler field, with B_w and λ_w the wiggler field amplitude and period, respectively. The parameter Φ is the phase of the electron in the beat wave formed by the wiggler and wave fields, with IFEL acceleration corresponding to positive values of $\sin\Phi$ and FEL radiation to negative values. The ability to choose the phase value Φ thus allows one to determine the output energy value and obtain minimal energy spreads on the output beam. Equation (1) is not an accurate description of the experimental situation, however, because of tapers in wiggler and guide magnetic fields introduced to allow smooth injection and stable interaction, as well as intrinsic large-orbit effects.

Components of the experiment described here, dubbed the microwave inverse free-electron laser accelerator (MIFELA) [11], include an rf gun and achromatic beam line as the injector, an rf structure for acceleration, a pulsed helical wiggler magnet, and a series of solenoid coils which provides an axial guiding magnetic field. An energy spectrometer and other diagnostics are also employed. A schematic depiction of the experimental layout is shown in Fig. 1, and the parameters of the experiment are summarized in Table I.

The MIFELA structure, a uniform stainless-steel circular waveguide operated near cutoff, also serves as the vacuum vessel and supports the conductors of the wiggler magnet, which are wound on its outer wall. The low waveguide refractive index increases the power density but also tightens the allowable tolerance on the waveguide inner radius; hence, machining constraints limited the overall length of the structure to less than 180 cm. rf power

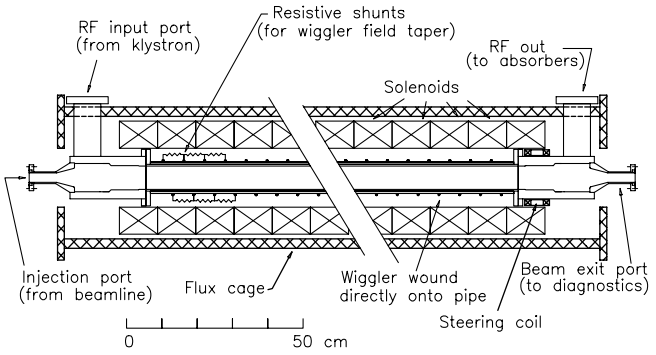

FIG. 1. Scaled drawing of MIFELA layout, showing rf waveguide, magnets, and beam path.

at 2.856 GHz is introduced into the waveguide through an input coupler which sets up the required TE_{11} rotating waveguide mode with greater than 97% circularity. Unused power is absorbed through a similar coupler at the MIFELA output, and incident and transmitted power levels can be measured with calibrated crystal detectors.

The wiggler field in MIFELA is provided by a bifilar helical winding which encircles the waveguide and which is pulsed with currents of up to 60 kA from a capacitor bank, helping to overcome eddy-current shielding by the conducting wall. As the electron energy increases, the period of the wiggler is tapered from 11.75 cm initially to 12.3 cm at the end of the device; this increases the wiggler field by 5% over that length, from 1.15 to 1.30 kG, as shown in Fig. 2.

Before it is accelerated, the beam traverses an adiabatic entry region in which it is "spun up," acquiring transverse momentum but undergoing little or no energy change [12]. In this entry region, the wiggler and axial fields are smoothly tapered from zero to their full values over five wiggler periods, as shown in Fig. 2. A series of resistive shunts between the two windings of the wiggler gradually decreases the wiggler current and creates the required taper. Figure 2 also shows the measured field in the wiggler entry region. An adjustable axial magnetic field, provided by a series of 18 individually controlled solenoid coils surrounding the waveguide and wiggler, stabilizes the electron orbits. This guide field is also tapered smoothly up from zero in the entry region.

The beam injected into MIFELA is produced by a 2-1/2 cell rf gun operating at 2.856 GHz and consists of a train of 5 ps microbunches of about 10^8 particles each, with an energy near 6 MeV. rf power from a single XK-5 klystron is split between the gun and the accelerator structure using a variable splitter and phase shifter, so that phase stability between the beam pulse and the accelerating bucket is assured. The phase control also allows selection of the ponderomotive phase at which the beam is injected, with an inherent phase spread of less than $\pi/20$ rad. After exiting the gun, the beam travels through an achromatic beam line containing an energy selection slit, which reduces the energy spread on the injected beam to the 1% level. Diagnostics on the beam line include toroidal current monitors and phosphor screens.

After acceleration, a pulsed steering magnet returns the spiraling beam to the axis. The beam's energy distribution is measured with a magnetic spectrometer, the beam being collected in a Faraday cup after passing through a 3 mm slit. Calculations and comparison with beam line data indicate a smallest resolvable energy change in the spectrometer of roughly 70 keV.

TABLE I. MIFELA parameters.

Scale parameters	
Entry region length	59 cm
Acceleration region length	105 cm
rf parameters	
Frequency	2.856 GHz
Drive power	3–7 MW
Pulse length	2 μs
Waveguide mode	TE_{11}
Polarization	Circular
Waveguide radius	3.14 cm
Waveguide refractive index $n = ck/\omega$	0.191
Wiggler parameters	
Winding radius	3.84 cm
Winding period	11.75–12.33 cm
Magnetic field on axis	1.15–1.3 kG
Axial guiding field	1.58 kG
Beam parameters	
Initial energy	5.1–6.1 MeV
Peak current	$\leq$0.3 A
Micropulse length	5 ps
Maximum orbit radius	6 mm

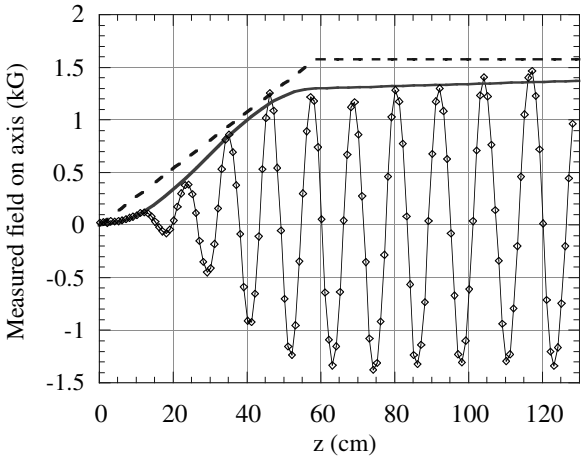

FIG. 2. Magnitudes of the axial (dashed line) and wiggler (solid line) magnetic fields vs axial position in MIFELA, compared with normalized benchtop dc measurement of the x projection of the wiggler field on axis (data points with interpolated line). Both entry and acceleration regions are shown.

Extensive simulations of the experiment were performed using the three-dimensional particle code ARACHNE [13], in which each particle is tracked individually and space charge is included, and which has been benchmarked against FEL experiments [14]. Simulation results guided the design of the experiment and have also been used below for comparisons with experimental data.

To observe acceleration or deceleration, spectra without the wiggler field were compared to spectra with the wiggler energized under otherwise identical conditions, since (as expected) no energy change was observed unless both wiggler and rf fields were present. Figure 3 shows output spectra obtained at two different phase values, 155° apart, taken with an input beam energy of 5.62 MeV, current of 80 mA, and rf power of about 6 MW. The initial value of the wiggler field was 1.3 ± 0.1 kG, with the axial field flat at 1.58 kG. (Note that phase values here are only relative.) Figure 3(a) (taken at 6°) shows an acceleration of 0.34 MeV, with an uncertainty of roughly 0.04 MeV, and clear separation between the unaccelerated and accelerated spectra. No unaccelerated particles are detected. While there is beam loss on the order of 30%, the energy distribution is nevertheless consistent, and the effective acceleration gradient is 0.43 MV/m. The percentage energy change of 6% for all exiting particles exceeds all prior measurements reported for IFELs.

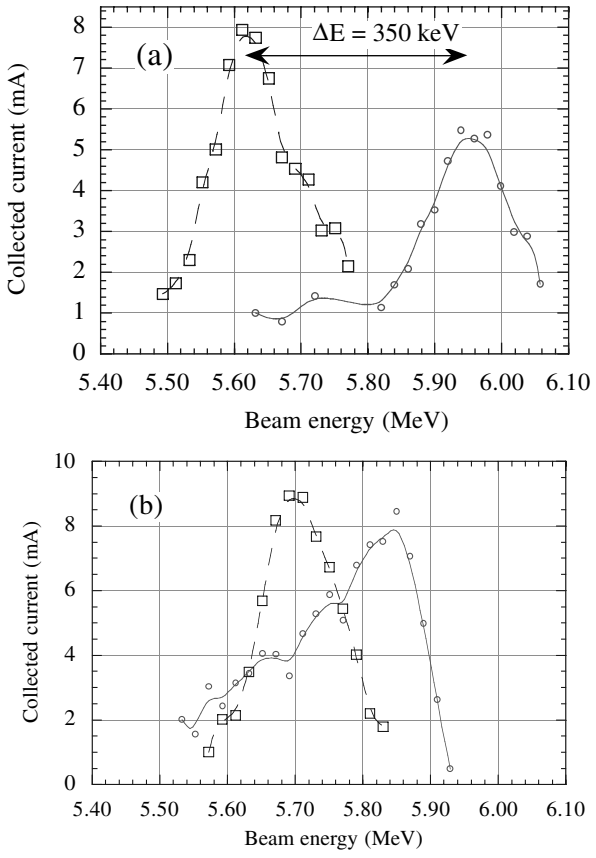

FIG. 3. Experimental energy spectra for two injection phases, both comparing the exiting beam spectrum under MIFELA operation (solid line, circles) with the spectrum in the absence of wiggler fields (dashed line, squares). (a) Injection phase of 6° (i.e., accelerating phase). (b) Injection phase of 161° (decelerating phase).

The plot in Fig. 3(b) (for a phase of 161°), with a distorted spectral shape in which the average and peak energies differ, is harder to interpret. Since the tapered wiggler field breaks the symmetry between accelerating and decelerating phases suggested by Eq. (1), the energy change is not expected to be equal and opposite to that for 6°; however, the observed peak is shifted in the positive direction, with an average energy gain comparable to the sensitivity limit of the spectrometer.

Both of these cases are compared with simulation in Fig. 4, where calculations assume a zero-emittance injected beam with nonzero energy spread. The resulting accelerated-beam spectrum is quite consistent with the experimental data, while the decelerating phase match is not as good; in the latter case, both spectral shape and peak location differ from their experimental values. However, the simulation does show increased energy width, greater beam loss, and distorted energy distribution for the decelerating phase as compared to the accelerating phase; asymmetry in the gain curve is also present. We believe that this shows an overall lack of orbit stability in the decelerating-phase case, when the wiggler taper no longer matches the beam energy gain, and that the resulting sensitivity of the beam to exact field and injection conditions would make its simulation less reliable.

Figure 5 shows output beam energy as a function of relative phase for an input rf power of 3 MW, a wiggler current of 30 kA producing an initial field of 1.1 ± 0.1 kG, and an axial field of 1.58 kG. The beam energy at input was 5.24 MeV, with a peak injected current near 40 mA. The maximum energy gain in this case is 0.20 ± 0.02 MeV, occurring here at a phase value near 30°. Again, there is asymmetry, with results for "decelerating" phases being

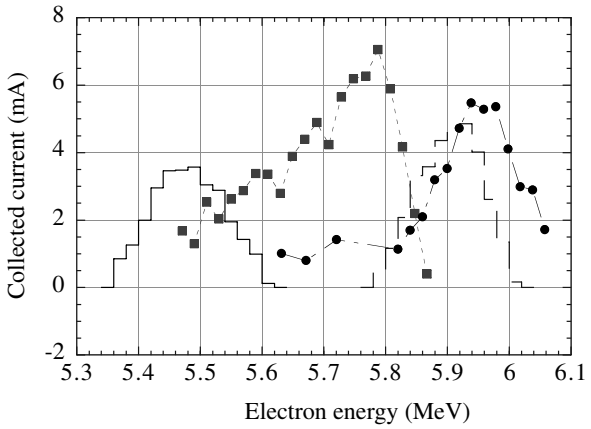

FIG. 4. Output energy spectra from Figs. 3(a) and 3(b) (solid circles and squares, respectively) compared with simulation using injected beam energy of 5.62 MeV, 6 MW rf power, and 1.25 kG of wiggler field (dashed and solid lines).

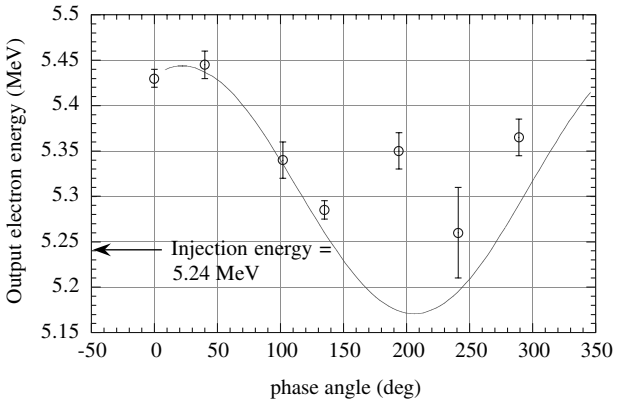

FIG. 5. Experimental plot of output beam energies (data points) for an input beam energy of 5.24 MeV and varying injection phases, compared with simulation (solid line). Error bars denote the uncertainty in the identification of output energy values, due to wide energy spread or multiply peaked spectra.

both mostly positive (although near zero) and less clean than results for accelerating phases. The error bars give an indication of the uncertainty involved in assigning a single number to the energy in each case, due to nonuniform energy spreads and instrumental noise.

Simulation results for the same conditions are shown in the figure as well, using a monoenergetic input beam with rms transverse emittance $\varepsilon_{x,y} = 14\pi$ mm mrad. Agreement is clear for accelerating phases (those less than 180°), though less precise in decelerating phases, showing once more the decreased beam quality and IFEL performance observed in that case.

In summary, these low-power results show general consistency with theoretical expectations, and close agreement between data and simulation has been demonstrated for accelerating phases, which are the cases of interest for IFELs. If we consider millimeter-wave IFELs at higher power levels and frequencies, approximate scaling laws derived from Eq. (1) and confirmed by simulation imply, for example, that a MIFELA operated with 150 MW of input power at a frequency of 34 GHz (parameters which have been proposed for next-generation rf accelerators [15]) should have a gradient of 30–35 MV/m. Our confirmation of the three-dimensional analysis with experimental data at large orbits also bolsters the case for a high-energy IFEL previously analyzed with a one-dimensional model [2]. Taking $\lambda_s = 10.6$ μm, $E = 12.5$ GeV, $\lambda_w = 6$ m, and $B_w = 1$ T, the electron orbit radius is roughly 2 mm, comparable to that in the current experiment and to the waist radius of the high-intensity optical field. A tapered wiggler, which keeps a_w constant, will suppress the increase of synchrotron radiation with increasing electron energy, but results in an increasing orbit radius. This research, in which the driving field also varies across the electron orbit, confirms the applicability of three-dimensional theory to IFELs at high energy.

The authors acknowledge the assistance of Mei Wang and M. A. LaPointe, helpful conversations with A. K. Ganguly and S. Y. Park, and technical advice from M. Shapiro and S. H. Gold. This work was supported by the U.S. Department of Energy, Division of High Energy Physics.

*Email address: rodney.yoder@yale.edu

[1] R. B. Palmer, J. Appl. Phys. **43**, 3014 (1972).
[2] E. Courant, C. Pellegrini, and W. Zakowicz, Phys. Rev. A **32**, 2813 (1985).
[3] C. Pellegrini and I. E. Campisi, in *Physics of High Energy Particle Accelerators,* edited by M. Month, AIP Conf. Proc. No. 105 (AIP, Woodbury, New York, 1983), p. 1058.
[4] I. Wernick and T. C. Marshall, Phys. Rev. A **46**, 3566 (1992).
[5] A. van Steenbergen, J. Gallardo, J. Sandweiss, and J.-M. Fang, Phys. Rev. Lett. **77**, 2690 (1996).
[6] Y. Liu *et al.,* Phys. Rev. Lett. **80**, 4418 (1998).
[7] W. Kimura (private communication).
[8] L. R. Elias *et al.,* Phys. Rev. Lett. **36**, 717 (1976).
[9] R. W. Warren *et al.,* IEEE J. Quantum Electron. **QE-19**, 391 (1983).
[10] T. B. Zhang and T. C. Marshall, Phys. Rev. E **50**, 1491 (1994).
[11] J. L. Hirshfield *et al.,* Nucl. Instrum. Methods Phys. Res., Sect. A **358**, 129 (1995).
[12] T. B. Zhang and T. C. Marshall, Nucl. Instrum. Methods Phys. Res. A **375**, 515 (1996).
[13] A. K. Ganguly and H. P. Freund, Phys. Rev. A **32**, 2275 (1985); **34**, 1242 (1986).
[14] D. E. Pershing, R. H. Jackson, H. Bluem, and H. P. Freund, Nucl. Instrum. Methods Phys. Res., Sect. A **304**, 127 (1991).
[15] M. V. Fazio, in *Advanced Accelerator Concepts, Eighth Workshop, Baltimore, 1998,* edited by W. Lawson, C. Bellamy, and D. F. Brosius, AIP Conf. Proc. No. 472 (AIP, New York, 1999), p. 220.